STEEL FIBRE REINFORCED SELF-COMPACTING CONCRETE FOR GRID FOUNDATIONS OF SINGLE-FAMILY HOUSES

N. Alves[*], J. Barros[*], A. Nunes[†] and L. Lourenço[*]

[*] Dep. Civil Eng., School Eng., University of Minho
Campus de Azurém 4800-058 Guimarães, Portugal
e-mail nunomartinsalves@msn.com, barros@civil.uminho.pt, lucio@civil.uminho.pt

[†] SECIL, Companhia Geral de Cal e Cimento, S.A.
Outão, 2901-864, Setúbal, Portugal
e-mail: angela.nunes@secil.pt

Keywords: Steel fibre reinforced self-compacting concrete; flexural and shear reinforcement; FEM; material nonlinear analysis; post-cracking tensile behaviour.

Summary: *This paper describes the preliminary studies carried out in the scope of an applied research project for the design and construction of Steel Fibre Reinforced Self-Compacting Concrete (SFRSCC) grid foundations for single-family houses. Adopting a constitutive model for the simulation of the post-cracking behaviour of fibre reinforced concrete, and modelling a complete typical single-family house by taking into account the soil-structure interaction, it was estimated the post cracking residual tensile strength for the SFRSCC to be developed. The aimed SFRSCC was prepared in a concrete mix plant, and standard specimens, ½ scale beam prototypes and a ¼ scale grid prototype were cast. To take into account, in the design context, the fibre distribution and orientation that can occur in grid foundations, core samples were extracted from distinct locations and depths in these beams, and the stress-crack width relationship, σ-w, was experimentally assessed. Based on the obtained σ-w curves, and using a cross-section layer model, the flexural capacity of the grid foundation was evaluated. The obtained results show the suitability of SFRSCC for this type of structures.*

1 INTRODUCTION

Experimental and numerical studies have shown that discrete steel fibres can replace conventional reinforcement in applications with redundant supports, such is the case of structures supported on soil [1]. Depending on the post-cracking residual strength of Fibre Reinforced Concrete (FRC), the ultimate load of these structures can be much higher than the load at crack initiation, and the maximum crack width at serviceability limit state conditions can be controlled in order to fulfil the requirements imposed by design codes. The use of FRC in structural applications is still, however, very limited, mainly due to the difficulties of including in the design models the influence of fibre distribution and fibre orientation that exist in real applications [2-5]. In the present paper the use of SFRSCC for a grid foundation of a typical single-family house is explored, being the preliminary studies of an applied research project that aims to develop and optimize SFRSCC, as well as a design strategy that takes into account the fundamental properties of the SFRSCC that are intrinsically dependent of its fresh properties, casting process and geometry of the grid. For this purpose, the cross section dimensions of the grid were pre-designed by performing numerical simulations with a computer program, based on the finite element method (FEM), able to model all the structural components of the building, as well as the soil-structure

interaction. Using a cross section layer model [6] capable of simulating the post-cracking behaviour of FRC materials, the post-cracking residual tensile strength necessary to attend the maximum bending moments actuating in the SFRSCC grid was determined. Adopting these characteristics for the post-cracking behaviour of the SFRSCC, a material nonlinear analysis was performed with the same FEM-based computer program, but now adopting a 3D smeared crack model capable of simulating the crack initiation and crack propagation in this type of elements. A cost competitive SFRSCC was then developed in a concrete mix plant, and concrete beams and standard specimens were cast. Core samples were extracted from distinct positions along the beams and at different depths in the cross section. These specimens were subjected to indirect tensile tests executed with the loaded plane making distinct angles with the longitudinal axis of the beam in order to assess the influence of the fibre distribution and orientation in the stress-crack opening relationship (σ-w). The σ-w obtained from these tests were compared with those determined from three point notched beam bending tests that were performed according to the recommendations of the CEB-FIP Model Code (MC) 2010 [7, 8]. This comparison has de purpose of verifying how the σ-w derived from this standard test is applicable for the design and quality control purposes of the SFRSCC grid foundations of single-family houses.

2 PREDICTION OF THE GRID INTERNAL FORCES FROM FEM-BASED ANALYSIS

2.1 The single-family houses concept, FEM model and loading conditions

Figure 1 represents the geometry of the structural system of the single-family houses to be simulated, which is composed by two floors supported in three RC frames in the x direction and four RC frames in the y direction. The columns transfer their loads to a SFRSCC grid foundation, whose study is the main objective of the present research program. The grid foundation, with a cross section of 600×600 mm^2, is supported on soil, and three distinct values of the soil reaction modulus [9] were considered (10, 50 and 90 MPa/m) to assess the influence of a low, moderate and high stiff soil in the internal forces of the SFRSCC grid. In all the numerical simulations, the beams and the columns of the RC frames were simulated with 3D Timoshenko finite elements with a Gauss-Legendre scheme integration rule of 1×2, the grid was modelled by 8 nodes solid finite elements with a Gauss-Legendre scheme integration rule of 2×2, and the soil was simulated as springs orthogonal to the bottom surface of the grid (it was neglected the stiffness contribution of the soil in contact with the lateral faces of the grid). Due to the relative low soil pressure expected for this type of structural problem, a linear and elastic behaviour was assumed for the springs working in compression, and a null contribution of the soil is considered when the springs become in tension. The membrane stiffness provided by each panel of the slab constituting the two floors was simulated by a X type truss structure connecting the nodes of the frames at the level of the floors. The load cases and load combinations considered in the performed analyzes are those recommended by the Eurocode 2 [8, 9], having been considered the most unfavourable wind and earthquake conditions that can occur in the Portuguese territory.

2.2 Linear and elastic analysis

A linear-elastic analysis was performed in order to obtain a preliminary evaluation of the maximum bending moments and shear forces in the grid components. For this analysis it was considered a concrete with a Young Modulus of 30 GPa and a Poisson coefficient of 0.15. From the obtained results it was verified that the maximum soil pressure is lower than 100 kPa, the maximum vertical displacement in the soil and in the structure does not exceed 7.5 mm, and the maximum differential settlement of the structure is limited to 1 mm, which according to European design codes are below the acceptable values for this type of structure. From the diagrams of the bending moments in the beams that form the grid foundation, a maximum design bending moment of 108 kN.m was obtained under the inner columns (positive values means tensile stresses in the face of the grid in contact with the soil), while between columns the maximum bending moment was -79kN.m. A maximum design shear force of 202 kN was registered near the inner columns. These maximum values were used to

estimate the post-cracking residual strength of the SFRSCC developed for the grid foundation.

2.3 Material nonlinear analysis

Since principal tensile stresses higher than the tensile strength have occurred in the grid foundation, a FEM-based nonlinear analysis was carried out, capable of simulating de post-cracking behaviour of the SFRSCC. Therefore, considering the maximum internal force values obtained in the linear elastic analysis, the SFRSCC post-cracking tensile residual strength was estimated by matching the maximum actuating bending moment with the flexural resistance of the foundation cross section, considering SFRSCC's with different residual tensile strength. This analysis was performed by the computer program DOCROS [6]. Adopting the diagram represented in Figure 2a for the simulation of the post-cracking behaviour of the SFRSCC, which has a residual strength parameter, μ, that defines the level of the residual strength between a crack width range of 0.1 to 2.5 mm, the relationship between μ and the normalized flexural resistance, M_{Rd}/M_{cr}, (where M_{Rd} and M_{cr} are the resisting and the cracking moment, respectively) was determined, which is represented in Figure 2b. To suppress completely the need of longitudinal reinforcement, there would be necessary a residual tensile strength of 0.53 (53% of the tensile strength), Figure 2b. However, if $\mu=0.4$ is considered, a SFRSCC of lower content of fibres can be adopted with conventional reinforcement in very low percentage (three bars of 6 mm diameter) applied in the bottom face of the grid foundation in the zones of the inner columns, Figure 4, resulting a competitive reinforcing solution.
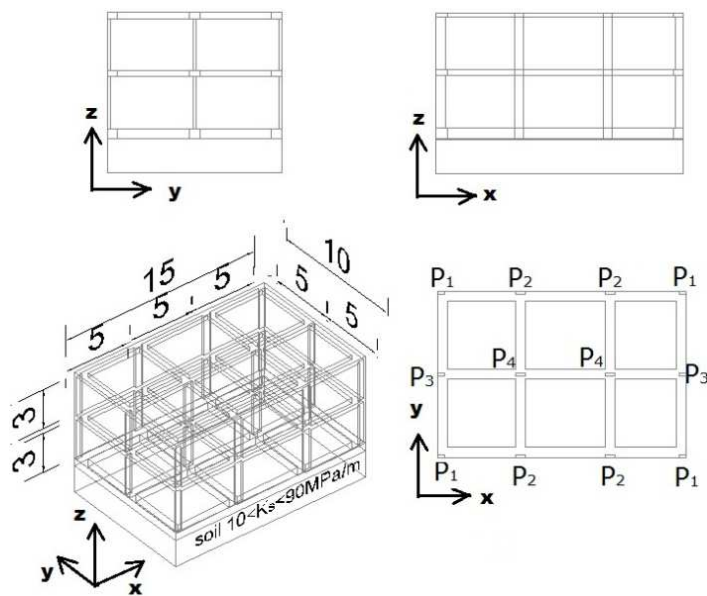

Figure 1: Model geometry of the typical single-family house (dimensions in meters)
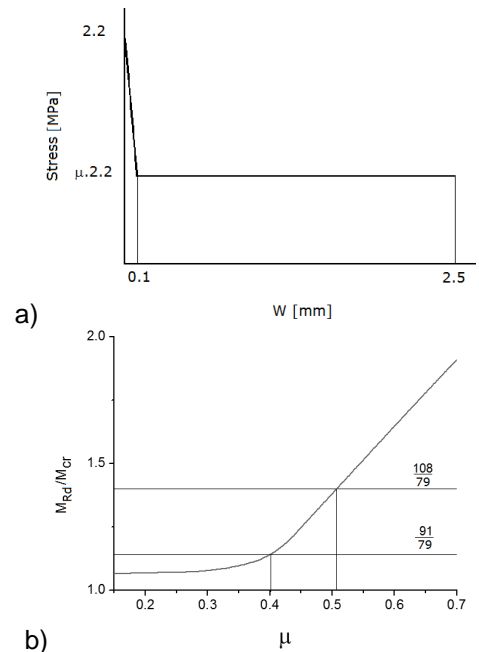
Figure 2: a) Diagram to simulate the post-cracking behaviour of SFRSCC, and b) normalized flexural resistance versus μ

Adopting a 3D multidirectional smeared crack model implemented into FEMIX v 4.0, whose details are described elsewhere [11], the stress redistribution in the grid foundation due to crack formation and propagation was assessed. The fracture mode I was simulated by the σ_n^{cr} - ε_n^{cr} diagram represented in

Figure 3, transforming the σ-w diagram of Figure 2a (with μ=0.4) in a σ_n^{cr} - ε_n^{cr} , by using the concept of crack band width, l_b. The values of the parameters of this constitutive model are indicated in Table 1. Due to the relatively reduced volume of SFRSCC that becomes cracked, small stress redistribution has occurred due to crack initiation and propagation, and the maximum bending moment remained almost unchanged.
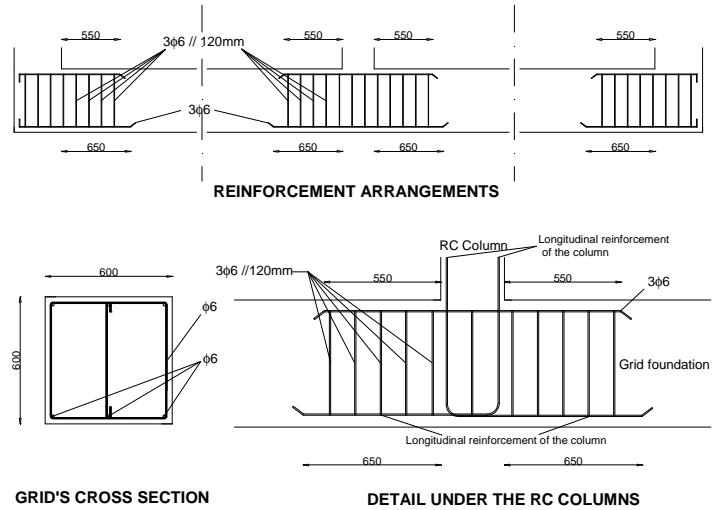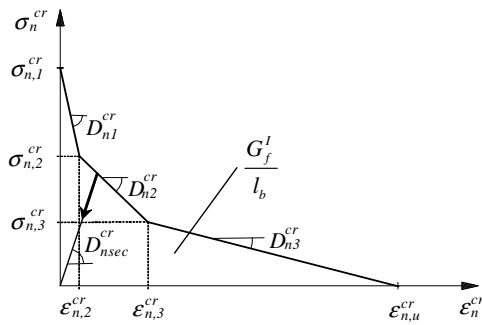

REINFORCEMENT ARRANGEMENTS

GRID'S CROSS SECTION   **DETAIL UNDER THE RC COLUMNS**

Figure 3: Trilinear stress-strain diagram for modelling the fracture mode I (G_f^I is the mode I fracture energy)

Figure 4: Arrangements of the conventional reinforcement in the grid foundation (dimensions in mm)

Table 1: SFRSCC properties used in the material nonlinear numerical simulations

Poisson's ratio	$v = 0.15$
Young's modulus	$E_c = 30000 MPa$
Compressive strength	$f_c = 48 MPa$
Trilinear tension softening diagram	$f_{ct} = 2.2 MPa$; $G_f^I = 4 MPa.m$; $\xi_1 = 0.05; \alpha_1 = 0.4$; $\xi_2 = 0.75; \alpha_2 = 0.4$
Parameter defining the mode I fracture energy available to the new crack [1]	$p_2 = 2$
Shear retention factor [1]	*Exponential* ($p_1 = 2$)
Crack bandwidth [1]	*Cubic root of the volume of the integration point*
Threshold angle [1]	$\alpha_{th} = 30º$

$\alpha_1 = \sigma_{n,2}^{cr} / \sigma_{n,1}^{cr}$, $\alpha_2 = \sigma_{n,3}^{cr} / \sigma_{n,1}^{cr}$, $\xi_1 = \varepsilon_{n,2}^{cr} / \varepsilon_{n,u}^{cr}$, $\xi_2 = \varepsilon_{n,3}^{cr} / \varepsilon_{n,u}^{cr}$ (see Figure 3); [1] [11]

2.4 Longitudinal and shear reinforcement

To control the crack width in FRC elements under bending, the second volume of the CEB-FIP MC 2010 [8] recommends the use of a cross sectional area of longitudinal steel bars given by the following equation:

$$A_{s,\min} = k_c\, k\, \left(f_{ctm} - f_{Ftsm} \right) \frac{A_{ct}}{\sigma_s} \tag{1}$$

where

k_c is a coefficient that takes into account the nature of the stress distribution within the section immediately prior to cracking and of the change of the lever arm. The equations for the evaluation of k_c are given in the prEN 1992-1-1 [10];

k is the coefficient that considers the effect of non-uniform self-equilibrating stresses, which lead to a reduction of restraint forces. The recommending values are indicated in the prEN 1992-1-1 [10];

f_{ctm} is the average value of the tensile strength of the FRC;

A_{ct} is the area of concrete within the tensile zone. The tensile zone is that part of the section which is calculated to be in tension just before the formation of the first crack;

σ_s is the absolute value of the maximum stress permitted in the reinforcement immediately after formation of the crack. This may be taken as the yield strength of the reinforcement, f_{yk};

f_{Ftsm} is the average value of the residual strength of the FRC. The equations for the evaluation of this parameter are given in the first volume of the CEB-FIP MC 2010 [7].

Therefore, applying Eq. (1) and considering three steel bars of 6 mm diameter and f_{yk}=500 MPa, the SFRSCC to be developed should have a f_{Ftsm} higher than the following value:

$$f_{Ftsm} = f_{ctm} - \frac{A_{s,\min}\, \sigma_s}{A_{ct}\, k_c\, k} = 2.2 - \frac{84.8 \times 500}{600 \times 300 \times 0.4 \times 0.8} = 1.46\,\text{MPa} \tag{2}$$

According to the second volume of the CEB-FIP MC 2010 [8], the shear resistance of a FRC beam that has longitudinal reinforcement can be determined from the following equation:

$$V_{Rd} = V_{Rd,s} + V_{Rd,F} \le V_{Rd,\max} \tag{3}$$

where the equations for the evaluation of the contribution of the steel stirrups and to avoid crushing of the compression struts are given in the prEN 1992-1-1 [10]. The term $V_{Rd,F}$ represents the contribution of the FRC for the shear resistance and is obtained from equation:

$$V_{Rd,F} = \left\{ \frac{0.18}{\gamma_c} \cdot k_d \cdot \left[100 \cdot \rho_l \cdot \left(1 + 7.5 \cdot \frac{f_{Ftuk}}{f_{ctk}} \right) \cdot f_{ck} \right]^{\frac{1}{3}} + 0.15 \cdot \sigma_{cp} \right\} \cdot b_w \cdot d \tag{4}$$

where [7]:

γ_c is the partial safety factor for the concrete (1.5);

k_d is a factor that takes into account the size effect and is equal to:

$1 + \sqrt{\dfrac{200}{d}} \le 2.0$ with d being the effective depth of the cross section in mm;

ρ_l is the reinforcement ratio of the longitudinal reinforcement, equal to $\rho_l = A_{sl}/b_w d$, being the A_{sl} [mm^2] the cross sectional area of the reinforcement which extends ≥ l_{bd}+d beyond the considered section (l_{bd} is the design anchorage length), and b_w [mm] is the smallest width of the cross-section in the tensile area;

f_{ctk} [MPa]   is the characteristic value of the tensile strength for the concrete matrix;

f_{ck} [MPa]   is the characteristic value of cylindrical compressive strength for the concrete matrix;

σ_{cp} [MPa] $= N_{Ed}/A_c < 0.2\, f_{cd}$ [MPa] is the average stress acting on the concrete cross section, A_c [mm^2], for an axial force N_{Ed} [N], due to loading or pre-stressing actions ($N_{Ed} > 0$ for compression);

f_{Ftuk} [MPa]   is the characteristic value of the ultimate residual tensile strength of FRC, that can be determined following the recommendations in the first volume of the CEB-FIP MC 2010.

Therefore, applying Eqs. (3) and (4) and considering γ_c =1.5, k_d=1.6, ρ_l =2.57e-04, f_{ctk}=1.6 MPa, f_{ck}=20 MPa and σ_{cp} =0, the value of the f_{Ftuk} in order that $V_{Rd,F} \geq V_{Sd,\max}$ ($V_{Sd,\max}$ =202000 N), i.e. no stirrups are needed, should be:

$$\left\{ \frac{0.18}{1.5} \cdot 1.6 \cdot \left[100 \cdot 2.57e - 04 \cdot \left(1 + 7.5 \cdot \frac{f_{\text{Ftuk}}}{1.6} \right) \cdot 20 \right]^{1/3} \right\} \cdot 600 \cdot 550 > 202000 \tag{5}$$

$$f_{\text{Ftuk}} > 13.2 \text{MPa}$$

that is a too high value. Therefore in the critical shear zones steel stirrups will be applied in order to limit f_{Ftuk} to 1.0 MPa ($V_{Rd,F} = 97465N$). Applying vertical steel stirrups of three arms of 6 mm diameter, and assuming an inclination of 45 degrees for the critical diagonal crack:

$$V_{\text{Rd,s}} = \frac{A_{\text{sw}}}{p} \cdot z \cdot f_{\text{ywd}} \cdot \sqrt{2}/2 > 202000 - 97465$$

$$\frac{3 \times \pi \times 6^2/4}{p} \cdot 495 \cdot 435 \cdot \sqrt{2}/2 > 104535 \tag{6}$$

a spacing of 120 mm is obtained for the steel stirrups. Figure 4 displays the reinforcement solution considered for the grid foundation. Since the columns have in each face, at least, 3 bars of 10 mm diameter, these bars can be also used for the flexural resistance of the grid foundation in the columns zones. If this reinforcement solution is selected, only three steel bars of 6 mm diameter are added at the top surface of the grid foundation to support the steel stirrups.

3   EXPERIMENTAL RESEARCH

3.1 Specimens and SFRSCC mix composition

The adopted SFRSCC mix composition is shown in Table 2. To have a SFRSCC with properties as closest as possible to those that can be found in the real structural application, the SFRSCC was made in industrial conditions, in a concrete mix plant. The self-compacting requisites of the material were evaluated when the SFRSCC started being downloaded from the truck, by executing the inverted Abrams cone slump test, according to EFNARC recommendations [12]. A slump value of 720 mm was obtained without occurrence of segregation.

Table 2: SFRSCC mix composition

CEM II 42.5 R [kg/m^3]	Limestone filler [kg/m^3]	Water/cement ratio	Superplasticizer[1] [%]	Steel Fibres[2] [kg/m^3]	D_{max}[3] [mm]
350	150	0.38	1.5	45	12.5

[1]Sikaplast 898; [2]CrysoFibre steel fibres AC65: l_f=35mm; d_f=0.55mm; l_f/d_f=65; tensile strength=1300 N/mm^2; [3]Maximum dimension of the aggregates

3.2 Flexural tests with standard beams

Seven standard beam specimens with the dimensions of 150×150×600 mm[3] were cast to be tested at twenty-eight days, following the recommendations in Chapter 5.6 of the volume 1 of CEB-FIP MC 2010 [7]. The SFRSCC sample used to fill the moulds of these standard beams was collected by passing it from the mixing-truck to the pump and then to a wheelbarrow. Signals of segregation were visible in the SFRSCC when resting in the wheelbarrow, due to the unfavourable pumping conditions. From these tests it was obtained stress-CMOD curves obtained in the three point bending tests with standard notched beams are presented in Figure 7, where CMOD is the crack mouth opening displacement, and σ is the stress evaluated from the following equation:

$$\sigma_j = \sigma_{fl,j} = \frac{3}{2} \frac{F_j \, L}{b \, h_{sp}^2} \tag{7}$$

where F is the applied load, L is the span length of the standard beam (500 mm), b is the width of the beam's cross section (150 mm) and h_{sp} is the distance between the notch tip and top of the beam's surface (125 mm). From Eq. (7) the residual flexural tensile strength parameters, $f_{Rj} = \sigma_j$, can be determined by evaluating F_j for distinct $CMOD_j$ (0.5, 1.5, 2.5 and 3.5 mm). The average value of the maximum flexural tensile strength ($f_{flm,max}$) was 5.5 MPa, and the average, characteristic, and design values of the residual flexural tensile strength parameters are indicated in Table 3, where f_{R1} and f_{R3} are the residual strength parameters for $CMOD_1$=0.5 mm and $CMOD_3$=2.5 mm, respectively. Due to the relatively high values of the standard deviation and small number of specimens, the characteristic values are significantly lower than the corresponding average values. The design values, f_d, were obtained from the characteristic ones by applying the safety factor of 1.5 recommended by CEB-FIP MC 2010 [7].

3.3 Flexural tests with beams extracted from the grid prototype

To assess the influence, in terms of the SFRSCC post-cracking behaviour, of the SFRSCC flow conditions in a grid prototype assumed representative of the real grid foundation, a grid prototype with a scale four times smaller than the real one was filled with the developed SFRSCC (see Figure 5a). This grid prototype was cast by pumping, first in the centre, and then sequentially in each of the four corners of the grid, as indicated in Figure 5b. Due to the impossibility of maintaining a constant suitable low pumping flow in this grid prototype, the grid was filled by intermittent pumping steps. This casting process caused visible segregation of the material in the pumping zones, where excessive paste content was observed. Twenty-eight days after the grid prototype has been cast, twenty-four beams were extracted from the grid, as shown in Figure 5b. These beams have the dimensions and were prepared according to the recommendations in Chapter 5.6 of volume 1 of CEB-FIP MC 2010 for the characterization of the post-cracking behaviour of FRC [7]. From the σ-CMOD curves recorded in the three point bending tests with the beams extracted from the grid prototype an $f_{flm,max}$=6.2 MPa was obtained, and the average, characteristic, and design values of f_R parameters are included in Table 3. The larger number of specimens, and the smaller standard deviation have contributed to the high characteristic values of f_R in this series of tests, when compared to the previous ones. However, the dispersion of the individual responses is also very high, to which the segregation that was detected during casting process may have contributed. Since the scale of the grid prototype is ¼ of the real grid foundation, while the fibres and the maximum aggregates (d_{max}) are about half scale of the ones expected to be used in the real application, the flowability conditions in the grid prototype are expected to be more adverse than those foreseen to occur in the real application, which have contributed for the occurrence of segregation during casting. A micro-concrete of $d_{max}\cong$6 mm could have been produced, but hooked end steel fibres with a length of about 15 mm was not possible to find.

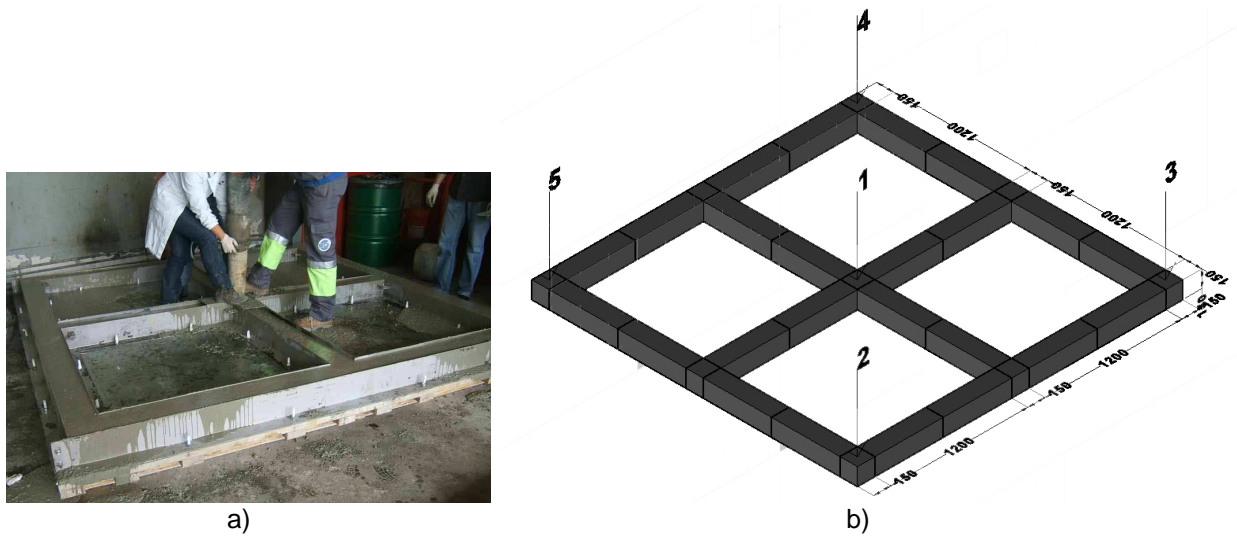a)   b)

Figure 5: a) The grid prototype; b) the casting sequence (1 to 5), and the beam cutting pattern
(dimensions in millimetres)

3.4 Indirect tensile tests

Aiming to assess the variation of the SFRSCC properties along an element of the grid, both in plant and in depth of the element, four beams were cast with a scale two times smaller than the elements that form the real grid foundation (see Figure 6). The moulds of these beams were levelled in the ground, and they were filled from their centre, by unloading the SFRSCC directly from the mixing-truck. Twenty-eight days after the beams have been cast, eight cylindrical cores were extracted from each beam according to the plan schematically represented in Figure 6. Each core was divided into three cylinder specimens of 100 mm high, in order to determine the stress-crack opening, σ-w, from indirect tensile tests. To assess the influence of the crack plan orientation (θ in Figure 6) on the σ-w relationship, notches were executed in the lateral faces of the cylinder specimens, with distinct orientation: 0º (the notched plane is orthogonal to the longitudinal axis of the beam), 30º and 45º. The width and depth of the notches were 5 and 10 mm, respectively.
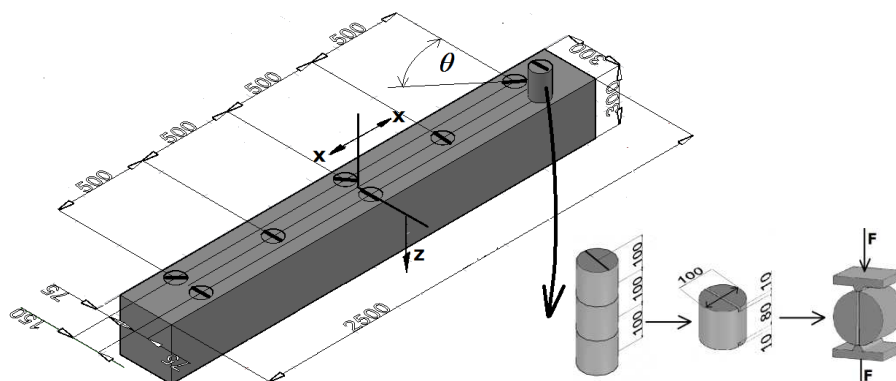

Figure 6: Dimensions of the beam prototypes, and localization of the specimens extracted for indirect tensile tests (dimensions in millimetres)

From these tests it was obtained the stress-crack width relationship for the specimens extracted from distinct depth in the cross sections of the beam prototypes. The stress is calculated from the following equation:

$$\sigma = \sigma_{sp} = \frac{2F}{\pi D\, L} \tag{8}$$

where *F* is the applied line load, *D* is the diameter of the specimen (100 mm) and *L* is the length of the net area in the notched plane (about 80 mm). Three distinct normalized depths (*z/h*) were analyzed (Figure 6), where *z* is the depth of the middle surface of the specimen and *h* is the height of the beam's cross section (300 mm). From the stress-crack width diagrams obtained in the indirect tensile tests it was obtained for the f_{R1} values ranging from 1.67 to 2.60 MPa, while for the f_{R3} the values varied between 0.90 and 1.34 MPa, which are much lower than the values determined from three point bending tests with standard beams and with beams extracted from the grid prototype. The average value of the maximum indirect tensile strength, $f_{spm,max}$, was 2.29 MPa, and the average, characteristic and design values of the residual strength parameters obtained from the σ-CMOD curves of the indirect tensile tests are included in Table 3. Due to the larger number of specimens (96) and smaller standard deviation, the characteristic and design values of the residual strength parameters were higher than those obtained in the flexural tests. The results have also indicated that for distances smaller than 1 meter from the casting point, the indirect tensile behaviour is almost the same. They have also indicated that for the dimensions of these beam prototypes the orientation of the fracture plane has marginal effect on the stress-crack width relationship of the extracted SFRSCC specimens.

Table 3: Average, characteristic and design values for the developed SFRSCC

	Flexural test		Indirect tensile test			Cylinder compression test
	Standard beams	Grid beams	z/h=0.17	z/h=0.50	z/h=0.83	
Nº of specimens	7	24	96			4
f_{R1m} [MPa]	5.3 (2.07)[1]	5.8 (1.43)	1.67 (0.62)	1.91 (0,62)	2.60 (0.62)	---
f_{R3m} [MPa]	4.34 (1.93)	5.24 (1.49)	0.90 (0.35)	0.92 (0.35)	1.34 (0.35)	---
f_{R1k} [MPa]	1.63	3.7	1.55	1.79	2.48	---
f_{R3k} [MPa]	0.92	3.02	0.825	0.85	1.27	---
f_{Ftsm} [MPa]	2.39	2.62	1.55	1.79	2.48	---
f_{Ftum} [MPa]	0.78	1.02	0.83	0.85	1.27	---
f_{Ftsk} [MPa]	0.74	1.67	1.55	1.79	2.48	---
f_{Ftuk} [MPa]	0.09	0.54	0.83	0.85	1.27	---
f_{ck} [MPa]	---	---	---	---	---	39
f_{cd} [MPa]	---	---	---	---	---	26.7
f_{Ftsd} [MPa]	0.49	1.11	1.03	1.19	1.65	
f_{Ftud} [MPa]	0.06	0.36	0.55	0.43	0.85	

$X_k = k.X_m$; $X_d = X_k/1.5$; [1]Coefficient of variation

3.6 Comparison of the results

In Figure 7a is represented the average curves for the stress-CMOD relationship obtained from the beams of the grid prototype (indicated as "Grid Beams"), standard beams, and from the specimens

9

extracted at distinct depth from the beam prototypes. In terms of average stress-CMOD relationship, the maximum post-cracking resistance was obtained in the bending tests from the beams extracted from the grid, while the minimum values were recorded in the indirect tensile tests in the specimens extracted from the beam prototypes. If the linear post-cracking constitutive model proposed by CEB-FIP MC 2010 is adopted to characterize the post-cracking behaviour of the SFRSCC, the diagrams represented in Figure 7b are obtained, where the parameters:

$$f_{Fts} = 0.45 f_{R1} \tag{9}$$

$$f_{Ftu} = f_{Fts} - \frac{w_u}{CMOD_3}(f_{Fts} - 0.5 f_{R3} + 0.2 f_{R1}) \geq 0 \tag{10}$$

are adopted for the beams, being w_u the maximum crack opening accepted in structural design, with a value that depends on the ductility required, having been adopted a value of 2.5 mm for the present application, while

$$f_{Fts} = f_{R1} \tag{11}$$

$$f_{ftu} = f_{Fts} - \frac{w_u}{CMOD_3} \cdot (f_{R1} - f_{R3}) \tag{12}$$

are considered for the indirect tensile tests, where w_u=2.5 mm. The design values of f_{Fts} and f_{Ftu} ($f_{Ftsd} = f_{Ftsk}/\gamma_f$ and $f_{Ftud} = f_{Ftuk}/\gamma_f$, where γ_f =1.5 according to CEB-FIP MC 2010 [7]) are indicated in Table 3. These results and the graphs of Figure 7 indicate that the stress-CMOD constitutive model with the highest residual strength was obtained from the indirect tensile tests, due to the relatively small coefficient of variation and the quite large number of tested specimens (96). This highlights the relevance of the minimum number of specimens to be carried out if quality control is based on the results determined from standard beams.
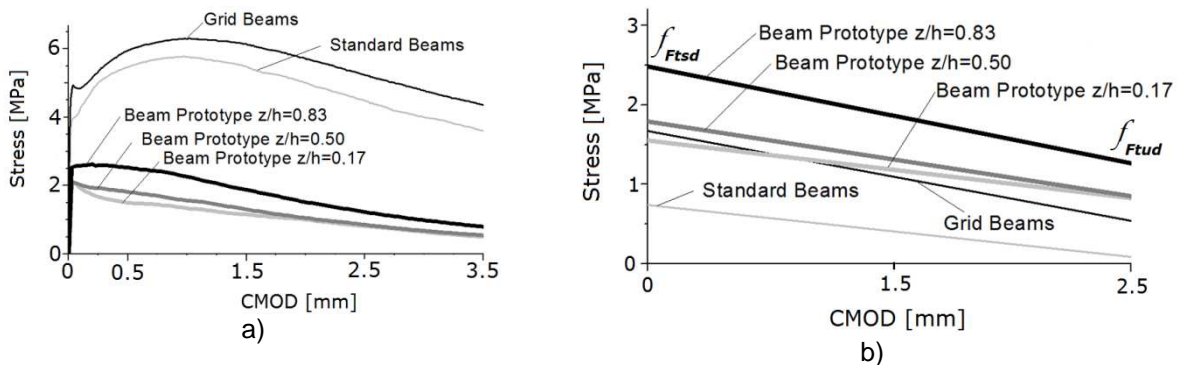

Figure 7: a) Average stress-CMOD curves; b) linear stress-CMOD constitutive model derived from the experimental tests according to the recommendations of CEB-FIP Model Code 2010

4   EVALUATION OF THE FLEXURAL RESISTANCE OF SFRSCC GRID FOUNDATION BASED ON THE EXPERIMENTAL RESULTS

Using the linear constitutive models, represented in Figure 7b, in the DOCROS program, distinct moment-curvature (M-χ) relationship were obtained for the cross section of the grid foundation: i) based on the constitutive models derived from the results of the standard beam tests and from the results of the beams extracted from the grid prototype (Figure 8a); ii) idealizing the cross section as composed by three layers (Figure 8b) and attributing to each layer the stress-crack width obtained from the indirect tensile tests carried out with specimens extracted from the corresponding normalized depth. For these approaches, the influence of the conventional reinforcement, represented in Figure 4, for the flexural resistance of the grid foundation was also analyzed. The M-χ relationship for these

analysis are represented in Figure 8c, where the maximum design values of the bending moments (positive and negative) obtained in Chapter 2 from the FEM-based material nonlinear analysis are also represented. Figure 8c shows that using the constitutive model derived from the tests with the specimens extracted from the beam prototypes, with or without conventional reinforcement, the positive and the negative resisting bending moments are larger than the corresponding actuating design bending moments. When using the constitutive model derived from the tests with the beams extracted from the grid prototype, only the situation without conventional reinforcement do not exceed the corresponding actuating design bending moment. However, using the constitutive model determined from the results of the tests with standard beams, the resisting bending moments are much lower than the corresponding actuating ones. Therefore, if standard notched beam bending tests are executed to derive the constitutive model for the design a FRC structure, of for the quality control purposes, a relatively large number of specimens should be tested in order to avoid a high penalization in the process of deriving design values from the tested data.
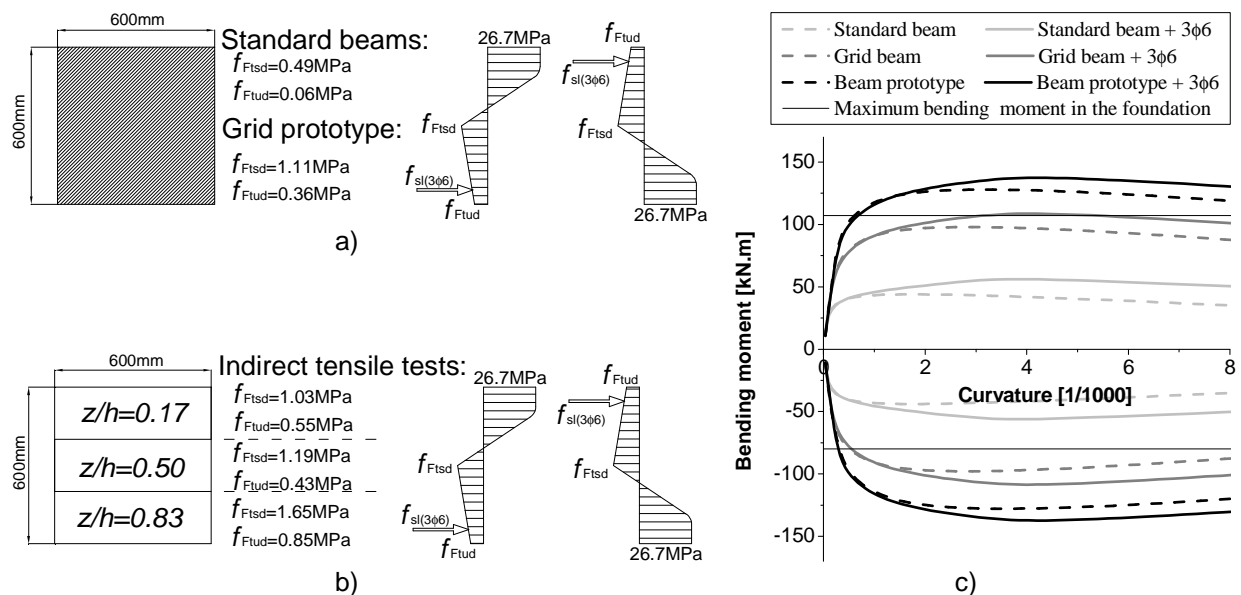

Figure 8: Constitutive model derived from the: a) bending tests, b) indirect tests; c) Moment curvature relationship from the application of these constitutive models for the SFRSCC grid foundation

5 CONCLUSIONS

This paper resumes the preliminary studies for the development and design of steel fibre reinforced self-compacting concrete (SFRSCC) for the grid foundation of a typical single-family house. Using a FEM-based computer program, able of simulating the complete structure and the soil-structure interaction, the maximum design bending moments ($M_{Sd,max}$) and shear forces ($V_{Sd,max}$) in the grid foundation were obtained, assuming a linear and elastic behaviour for all the intervening materials. Using a cross section layer model, capable of simulating the full nonlinear behaviour of SFRSCC, the post-cracking residual tensile strength of the SFRSCC to be developed was estimated, in order that the resisting bending moments (M_{Rd}) exceeds $M_{Sd,max}$. Using a 3D smeared crack model for solid finite elements available in the FEMIX computer program, and considering the soil-structure interaction with soils with a range of values for their properties than can be found in real applications, the bending and shear diagrams in the grid foundation were determined. Using these diagrams and the formulation proposed by the CEB-FIP model code 2010, the percentage of steel stirrups and the percentage of longitudinal reinforcement in the critical zones were evaluated. The SFRSCC was prepared in a mix

plant in order to follow, as closest as possible, the expectable conditions of the production of this material in real situations.

The second part of this paper is dedicated to the evaluation of the stress-crack width (σ-w) relationship for modelling the post crack behaviour of the developed SFRSCC. For this purpose, three experimental programs were carried out: one executing three point notched beam bending tests according to the CEB-FIP model code 2010 recommendations (designated standard tests); a second one by executing this type of tests with beams extracted from a grid prototype with a ¼ scale of the real grid foundation; and the third one by performing indirect tensile tests with samples extracted from distinct depth and locations in beam prototypes in order to assess the influence of fibre distribution and orientation in the σ-w relationship. Due to the relatively high coefficient of variation obtained in the standard tests, and the relatively small number of specimens in this experimental program, the σ-w constitutive law derived from the results of these tests conducted to a resisting bending moment (M_{Rd}) lower than the actuating bending moments (M_{Sd}) in the critical regions of the grid foundation. However, the σ-w derived from the other two experimental programs have assured M_{Rd}>M_{Sd} in all sections of the grid foundation. Therefore, if standard beams tests are used to develop the design constitutive model for the SFRSCC, or for quality control, a set of twelve specimens is recommended. If the fibres used in the present research are used in the real application the content of fibres should be increased in order to assure f_{Ftsm}>2 MPa and f_{Ftuk}>1 MPa, which seems attainable with a content of fibres around 60 kg/m^3. It can be concluded that SFRSCC can constitute an economic and technical competitive alternative for grid foundations of single-family houses, where conventional reinforcement is only applied below the columns, and can be integrated as part of the column reinforcement.

ACKNOWLEDGEMENTS

REFERENCES

[1] Barros, J.A.O.; di Prisco, M.; di Prisco, C., "Modelling FRC infrastructures taking into account the soil-structure interaction", Conf. on Numerical Methods in Engineering, Barcelona, Spain, 29 June to 2 July 2009.

[2] Cunha, V.M.C.F., "Steel fibre reinforced self-compacting concrete: from micro-mechanics to composite behaviour", PhD Thesis, University of Minho, May 2010.

[3] Wuest, J., "Comportement structural des bétons de fibres ultra performants en traction dans des elements composes", PhD thesis, Thesis n. 3987, EPFL, 2007. (in French)

[4] Tan, K-H., Paramasivam, P., Tan, K-C., "Cracking characteristics of reinforced steel fibre concrete beams under short- and long-term loading", Advanced Cement Based Materials, 2, 127-137, 1995.

[5] Oliveira, F.L., "Design-oriented constitutive model for steel fiber reinforced concrete", PhD Thesis, Universitat Politécnica de Catalunya, Barcelona, Spain, 2010.

[6] Basto, C.A.A.; Barros, J.A.O., "Numeric simulation of sections submitted to bending", Technical report 08-DEC/E-46, Dep. Civil Eng., School Eng. University of Minho, pp. 73, August 2008.

[7] CEB-FIP Model Code 2010, First Complete draft, First Volume, fib, March 2010

[8] CEB-FIP Model Code 2010, First Complete draft, Second Volume, fib, April 2010

[9] Bowles, J.E., "Foundation analysis and design", Fifth Edition, McGraw-Hill International Editions, Civil Engineering Series, 1997.

[10] prEN 1992-1-1 - Eurocode 2: Design of concrete structures - Part 1-1: General rules and rules for buildings, (2010)

[11] Gouveia, A.V.; Barros, J.A.O.; Azevedo, A.; Sena-Cruz, J.; "Multi-fixed smeared 3d crack model to simulate the behavior of fiber reinforced concrete structures", CCC 2008 - Challenges for Civil Construction, FEUP, Porto (2008).

[12] EFNARC; "The European Guidelines for Self Compacting Concrete". May 2005.